RSC Advances

ROYAL SOCIETY OF CHEMISTRY

www.rsc.org/advances

Mechanism Investigation on the Ag/SiN_x Firing-through Process of the Screen-Printed Silicon Solar Cells

Shiliang Wu,[1] Wei Wang,[1] Li Li,[1] Dong Yu,[1] Lei Huang,[1] Wenchao Liu,[2] Xiaoshan Wu,[1] and Fengming Zhang[1,*]

[1]*National Laboratory of Solid State Microstructures, Center of Photovoltaic Engineering and School of Physics, Nanjing University, Nanjing 210093, China.*

[2]*National Laboratory of Solid State Microstructures, Center of Photovoltaic Engineering and School of Modern Engineering and Applied Sciences, Nanjing University, Nanjing 210093, China.*

Abstract

The mechanism of Ag/SiN_x firing-through process in the manufacturing of multi-crystalline silicon solar cells has been studied. The firing temperature effect on the electrical performance of screen printed multi-crystalline silicon solar cells with conversion efficiency up to 17.2% has been investigated. It is revealed that with the increase of firing temperature both the series resistance and shunting resistance of the solar cells decrease monotonically, while the reverse leakage current rises gradually. SEM and EDX are used to study the cross-sections of the Ag/Si interface under the fingers and it is revealed that hexagonal like silver crystallites are formed due to the chemical reaction between the SiN_x and Ag_2O in the Ag paste during the firing process, through which the direct interconnection between the emitter and silver particles contained in the paste is achieved. The physical process of the firing-through has been discussed. Moreover, the diffusion coefficients of different temperature are obtained by fitting the diffusion profiles.

Key words: Multi-crystalline Si solar cell, Metallization, Screen printed process

[*]Corresponding author. E-mail address: fmzhang@nju.edu.cn

Introduction

In photovoltaic industry, screen-printing has been the most commonly used method to deposit metallic paste onto silicon with SiN_x for front metallization. In the large scale manufacturing of solar cells, a thin layer of SiN_x is needed to passivate the dangling bonds and reduce the light reflection at the front surfaces of the silicon wafers for increasing the light-electricity conversion efficiency. Silver fingers are then printed on the SiN_x layer for soldering in the inter-connection between cells for making modules. Due to the electrical insulation of the SiN_x, therefore, a so-called firing process is essential to drive the Ag through the SiN_x layer to have the carriers generated in the cells transmitted out. The firing process is a rapid annealing process at high temperature.[1]

For screen-printed solar cells, it is well known that the peak temperature in the firing process is extremely important to the performance of the solar cells. Particularly, the fill factor (FF) of the solar cell is strongly affected by both the series resistance and shunting resistance. As an important part of the series resistance, the contact resistance depends on the behavior of Ag/Si contact interface after the firing process.[2] In addition, the junction leakage and shunting characteristics are also heavily affected by the firing process. It has been concluded that in the manufacturing of solar cells, there exists an optimal firing temperature to reasonably ensure good front contact and low reverse leakage current for the junction.

The current commercial silver paste consists of silver particles, glass frit, solvents, binders and relevant oxides including Ag_2O etc. With firing, a good ohmic contact between the silver fingers and the emitter of the cells is formed. It is generally believed that with the increase of the reaction temperature, the SiN_x layer is gradually etched and a glass layer (mainly SiO_2) is formed between the emitter and the silver finger.[3] The glass layer at the interface is assumed to be insulating and is therefore responsible for high contact resistance. Up to now, two maim hypotheses have been proposed to explain the mechanism of current transport from the n-type emitter of silicon solar cells to the silver fingers: 1) the current is supposed to be transported via (local) direct interconnections between the silver fingers and the silicon,[4, 5] 2) the current is supposed to be transported via a multi-step tunneling process from the emitter to the silver fingers through the glass layer.[6, 7]

In fact, quite a few reports have been in trying to reveal the physical picture of the Ag/Si interface. Butler and his colleagues have investigated the contact potential between the Ag and Si interface both experimentally and theoretically, and it was found the Schottky Barrier height (SBH) depends upon the orientation of the Si surface.[8] By detailed work, including both observation of the microscopic structure of the formed front contacts on flat and textured mono–crystalline Si solar cell surfaces with SEM and measurement of the contact resistivity after sequential etch-back of the metallization from different silver thick film pastes, Cabrera et al presented convincing experimental evidence that the major current flow into the silver finger is through these direct contacts.[9,10] Moreover, some more works have studied the nanoscale silver crystals at the interface of silver thick film contacts on n-type silicon.[11-13]

Although the works mentioned above and presented in some other reports,[14-16] a complete and clear picture of the contact formation between silver and the Si emitter is still not available. Also, little work has been carried out quantitatively on the process of the current transport from the

emitter of the solar cells to the silver fingers and on the precise correlation between silver and the quality of the ohmic contact, especially no report on practical textured multi-crystalline solar cells has been found. Based on the cross-section observation with SEM, here presented is the first and preliminary investigation on the mechanism of the Ag/SiN_x firing-through process results of the influence of firing temperature to the electrical properties and the microstructure of the Ag/Si contact interface, giving a complete physical picture of the firing process.

Experimental

Samples of solar cells were fabricated on the typical industrial production line，using 156 ×156 mm^2 p-type polycrystalline silicon wafers. The wafers were first textured or saw damage-etched by acid etching using a mixture HNO_3/HF system. The emitter was formed by standard $POCl_3$ diffusion with 45 Ω/□ sheet resistance, and then the selective-emitter technology was used in order to obtain good cell performance. The SiN_x antireflection and passivation layer was deposited via PECVD with the average thickness 82nm and refractive index 2.08. The front and back metallization process was carried out by screen-printing commercial silver and aluminium pastes, respectively. Finally, the front and back contacts were simultaneously formed during a fast firing process in an IR heated belt furnace.

There were five groups of sample cells with firing temperatures of 745℃, 775℃, 805℃, 835℃, and 865℃, respectively, while the other preparation conditions were identical. The electrical performance of the sample cells was characterized with I-V tester. The field-emission scanning electron microscopy (SEM) and energy dispersive X-ray spectrometry (EDX) were used to study the cross-section of Ag/Si interface.

Results and discussion

Shown in the table are the results of the electrical performance of the sample cells. It can be noted from the table that the open circuit voltage (V_{oc}), shorted circuit current (I_{sc}) are almost the same, which is due to the consistently similar quality of the start wafer materials and identical manufacturing conditions except the firing temperature. Figure 1 (a) - (d) are the firing temperature dependence of the individual electrical parameters of efficiency and fill factor (a), series resistance (b), shunting resistance (c) and reverse leakage current (d), respectively.

It can be seen from Figure 1 (a) that with the rise of temperature the value increases first and turns to decrease after a peak is reached for both the conversion efficiency and fill factor. It is demonstrated that both the series resistance and shunting resistance decrease monotonically with the increase of firing temperature, as shown in Figure 1(b) and (c). As we know that the lower the series resistance is, the better the cell performs. Therefore, from the ohmic contact point, high firing temperature is desired. However, on the other hand, the too high firing temperature is harmful to the performance of cells because the over diffusion of silver into the surface region of the cells could cause higher probability of shunting at the junction. So, there exists an optimal firing temperature to compromise for the series resistance and shunting resistance, which has been indicated from Figure 1 (a). Figure 1 (d) is the dependence of the reverse currents at bias voltages of -10 V and -12 V, respectively on the firing temperature. Clearly, the reverse leakage currents increase with the rise of firing temperature. The fact of higher reverse current caused by the higher firing temperature is consistent with observation of firing temperature dependence of shunting

resistance as discussed above.

In order to better understand the effect of the firing temperature on the series resistance, shunting resistance and reverse leakage current, it is helpful to study the interface region formed by the diffusion of silver at different firing temperatures. Underneath the finger areas of sample cells obtained at different firing temperatures were analyzed with EDX. From the EDX data, the profiles of the silver diffusion into the surface areas were plotted as shown in Figure 2. As shown in Figure 2, the diffusion of silver mainly concentrates in the surface area of the emitter. Higher temperature corresponds to higher silver content and this is responsible for higher reverse leakage current and lower shunting resistance.

To fit the profile of the silver, it is supposed that the surface concentration of silver is unchanged in the firing process. According to the diffusion theory,[17] the diffusion concentration can be written as

$$N(x,t) = N_s erfc \frac{x}{2\sqrt{Dt}} \qquad (1)$$

where N_s is the surface concentration, D the diffusion coefficient, x the depth and t the time. From the profiles of different firing temperatures in Figure 2, the diffusion coefficient changes with firing temperature can be obtained and is shown in Figure 3.

While, as we know the diffusion coefficient can be written as

$$D = D_0 \exp(-\frac{E_a}{kT}) \qquad (2)$$

where D_0 is a pre exponential constant, $E_a$the activation energy, k the Boltzmann coefficient. For single crystalline silicon, according to the literature,[18] D_0= 1×10^{-3} cm^2/s, E_a=1.6 eV. Therefore, the temperature dependence of the diffusion coefficient can plotted from Equation (2) and the plotted line is also shown in Figure 3. Convincingly, the diffusion coefficient obtained from multi-crystalline silicon is nearly consistent to that from mono-crystalline silicon.

The cross sections of the silver diffused areas under the fingers of the sample cells obtained at different firing temperatures were further studied with SEM. Figure 4 (a) and (b) show the SEM cross-sectional images of the samples at 745℃ (a) and 805℃ (b), respectively. The big voids observed in the figures are due to the missing of the silver particles, caused during the sample preparation for cross section study. Although the non-flat interface due to the feature of the textured surface on the solar cells, it is clear that there exists a thin layer between the silver and the silicon. While it was revealed with EDX that there is a large amount of nitrogen (about 11.75atm% at the cross mark point) in the thin layer of the sample for Figure 4 (a), the EDX result is shown in the Figure 5. However, no nitrogen was detected in the thin layer of the sample for Figure 4 (b), in accordance with the previous studies.[19] It can be seen that for both cases in addition to the larger silver particles there are a lot of small hexagonal like crystallites embedded into the thin layers. Moreover, it can be found that the hexagonal like crystallites in Figure 4 (b) are larger than those in Figure 4 (a).

The interpretation of the interaction between the silver and the SiN_x thin layer before diffusing into the silicon is interesting and meaningful. For the larger silver particles located at the void

positions, they are obvious from the original paste. However, the small hexagonal like crystallites could only come from the reaction during the firing. From the EDX analysis of the sample for Figure 4 (b), the hexagonal like crystallites were found to be silver content, as shown in the Figure 6. According literature,[20] the most likely redox reaction seems to be:

$$2Ag_2O_{(in\ glass)} + SiN_{x(s)} \rightarrow 4Ag_{(s)} + SiO_{2(in\ glass)} + x/2N_{2(g)} \quad (3)$$

Therefore, the hexagonal like silver crystallites are formed due to the reaction of Ag_2O and SiN_x. It is known that firing at higher temperature could increase the aggressiveness of the etching reaction between the paste and the SiN_x layer. This could explain the relative larger silver crystallites in Figure 4 (b) than those in Figure 4 (a), due to the higher firing temperature of the samples for Figure 4 (b). It is also noted that for both the cases all hexagonal like silver crystallites are located at the interface between the larger silver particles and the emitter. With the increase of the reaction temperature, the SiN_x layer is gradually etched from the top surface and the original silver particles from the paste are immerged in the molten glass and at the same time the hexagonal like silver crystallites are nucleated and grow up at the reaction front between the Ag_2O and SiN_x. As long as the progressing of reaction, the reaction front moves closer to the emitter and so do the hexagonal like silver crystallites while they grow up. After the completion of the reaction, the SiN_x could be consumed up and all the hexagonal like silver crystallites reach destination at the emitter surface. However, because the glass composite are always in molten state at the reaction temperature, all the hexagonal like silver crystallites are imbedded in as shown in the figures. Finally, the good ohmic contact could be achieved through the electrical connection between the large silver particles and the emitter via the small hexagonal like silver crystallites, as shown schematically in Figure 4 (c). At the same time, it is reasonable that the silver crystallites grow up and the contact area becomes larger with the increase of the firing temperature. Consequently, with increasing firing temperatures, the series resistance reduces because better direct interconnection between the emitter and the silver finger is realized for larger contact area. However, higher temperature means more silver diffusion into the emitter, giving rise to higher chance for the junction area to be shunted. Therefore, the reverse leakage current would increase and the shunting resistance would decrease because of the more diffusion of the silver.

Conclusion

The firing temperature effect on the electrical performance of multi-crystalline silicon solar cells has been investigated. It has been found that with the temperature increase both the efficiency and fill factor increase and then decrease gradually after a peak value reached. The higher firing temperature could induce lower series resistance due to the larger contact area between the silver particles and the emitter. A clear picture of the firing process, i.e. the hexagonal like silver crystallites are nucleated and grow up at the reaction front between the Ag_2O and SiN_x with movement closer to the emitter, has been revealed. From the studies of microstructure, it is confirmed that the current transport mechanism is interconnections between the emitter and silver fingers via the hexagonal like silver crystallites.

Acknowledgments

We acknowledge support from NKPBRC (2010CB923404), NNSFC (Nos. 11274153, 11204124, 51202108).

References

1. E. Cabrera, Doctoral thesis, Constanz University, 2013.
2. K. Firor, S. J. Hogan, J. M. Barrett, and R. T. Coyle, Proceedings of the 16th IEEE Photovoltaic Specialists Conference, 1982, pp. 824–827.
3. G. Schubert, F. Huster and P. Fath, Sol. Energy Mater. Sol. Cells, 2006, 90, 3399–3406.
4. G. C. Cheek, R. P. Mertens, R. Van Overstraeten and L. Frisson, Trans. Electron Devices, 1984, 31 (5), 602-609.
5. R. J. S. Young and A. F. Carroll, Proceedings of the 16th EC PVSEC, Glasgow, 2000, pp. 1731-1734.
6. M. Prudenziati, L. Moror, B. Morten and F. Sirotti, Act. Passive Electr. Compounds, 1989, 13, 133-150.
7. T. Nakajima, A. Kawakami, A. Tada, Int. J. Hybrid Microelectron, 1983, 6 (1), 580-586.
8. K.T. Butler, P.E. Vullum, A.M. Muggerud, E. Cabrera and J.H.Harding. Phys. Rev. B, 2011, 83, 235307.
9. E. Cabrera, S. Olibet, J. Glatz-Reichenbach, R. Kopecek, D. Reinke, and G. Schubert, J. App. Phys., 2011, 110, 114511.
10. E. Cabrera, S. Olibet, J. Glatz-Reichenbach, R. Kopecek, D. Reinke and G. Schubert, Energy Procedia, 2011, 8, 540–545.
11. H. Yang, X. D. Lei, H. Wang and M. Q Wang, Clean Techn Environ Policy, 2013, 15, 1049-1053.
12. S. Kontermann, R. Preu and G. Willeke. Appl. Phys. Lett., 2011, 99, 111905.
13. S. Kontermann, A. Ruf, R. Preu and G. Willeke. Appl. Phys. Lett., 2012, 99, 121907.
14. P. Narayanan Vinod, RSC Advance, 2013, 3, 14106-14113.
15. S. Kontermann, G. Willeke and J. Bauer. Appl. Phys. Lett., 2010, 97, 191910.
16. P. Narayanan Vinod, RSC Advances, 2013, 3, 3618-3622.
17. L. R. Yan, W. Zhou and D. G. Liu, IC Fabrication, Tsinghua University Press, 2010, 68-69.
18. S. W. Jones, Diffusion in silicon, IC Knowledge LLC, April 25, 2008.
19. C. H. Lin, S. Y. Tsai, S. P. Hsu and M. H. Hsieh, Sol. Energy Mater. Sol. Cells, 2008, 92, 1011– 1015.
20. K. K. Hong, S. B. Cho, J. S. You, J. W. Jeong, S. M. Bea and J. Y. Huh, Sol. Energy Mater. Sol. Cells, 2009, 93, 898–904.

Table The electrical performance of solar cells with different firing temperatures.

T(℃)	I_{sc} (A)	V_{oc} (V)	FF(%)	E_{ff} (%)	R_s (Ω)	R_{sh} (Ω)	I_{rev1} (A)	I_{rev2} (A)
745	8.426215	0.624533	78.17645	16.90490	0.002056	210.8812	0.102252	0.418127
775	8.434872	0.624247	78.32449	16.94662	0.001990	149.0577	0.156951	0.511428
805	8.47421	0.626127	78.89935	17.20229	0.001923	138.2943	0.162102	0.521614
835	8.466094	0.621599	78.67301	17.01256	0.001840	106.0098	0.170251	0.536030
865	8.280422	0.623448	78.61310	16.67700	0.001720	62.11593	0.236446	0.963737

Figure Captions:

Figure 1. Temperature dependence of the electrical properties of the sample cells. (a) Fill factor (FF) and conversion efficiency (E_{ff}), (b) Series resistance (R_s), (c) Shunting resistance (R_{sh}) and (d) Reverse leakage current (I_{rev1} and I_{rev2} correspond to the bias voltage - 10V and - 12V).

Figure 2. Semi-logarithmic plot of the profiles of the silver diffusion in the surface of silicon.

Figure 3. Temperature dependence of the diffusion coefficients from experiment at different firing temperatures with comparison to the theoretical values for mono-crystalline silicon.

Figure 4. Cross-section images of the Ag/Si contact interface. (a) firing at 745℃, (b) firing at 805℃(the optimal firing condition) and (c) simple current transport model.

Figure 5. The analysis result of EDX at the cross mark point.

Figure 6. Elemental mapping of microstructure by EDX. (a) SEM image of the interface, (b) mapping of silicon and (c) mapping of silver.

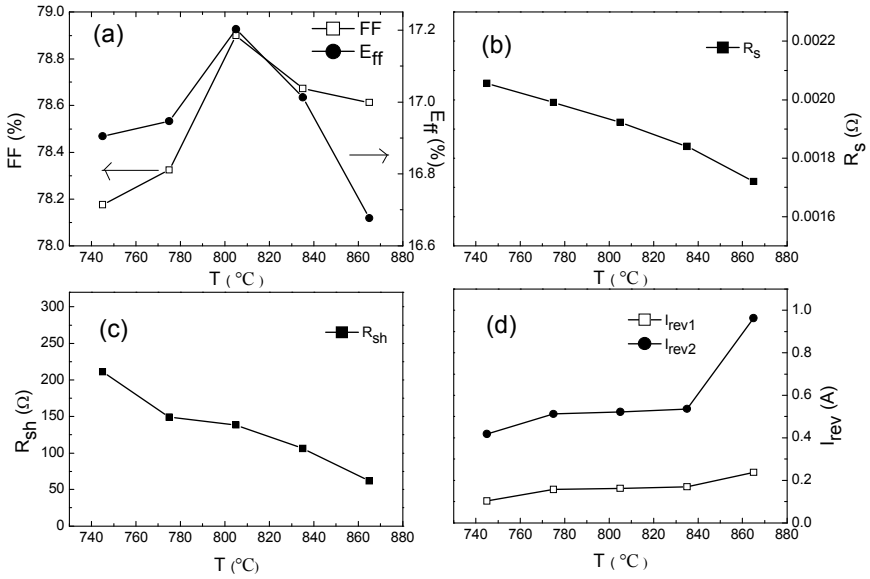

Figure 1

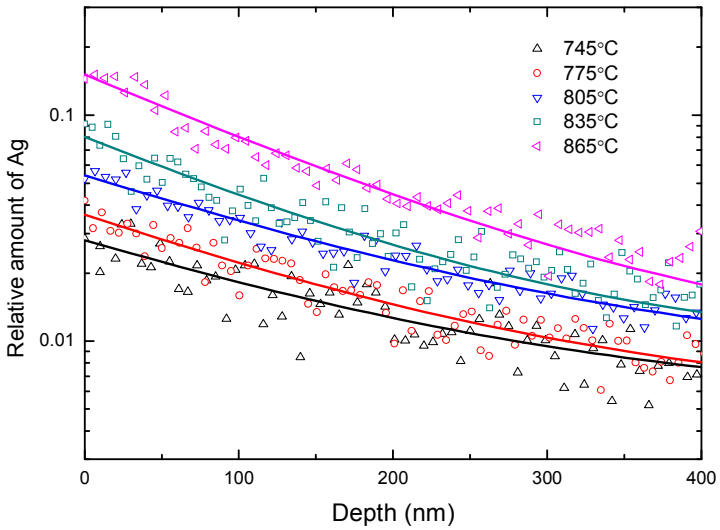

Figure 2

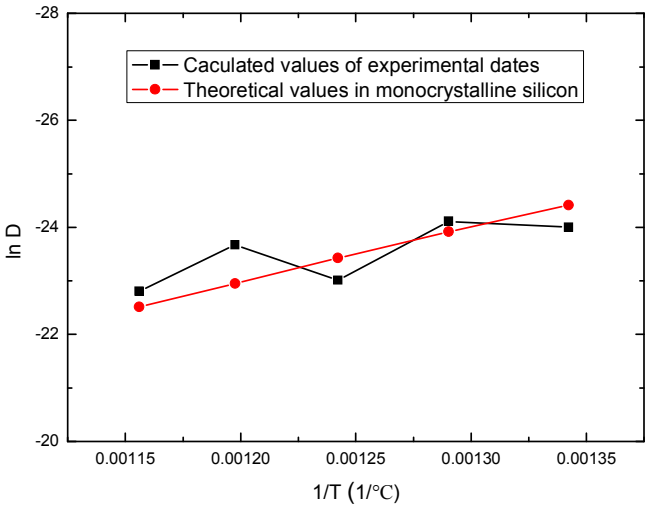

Figure 3

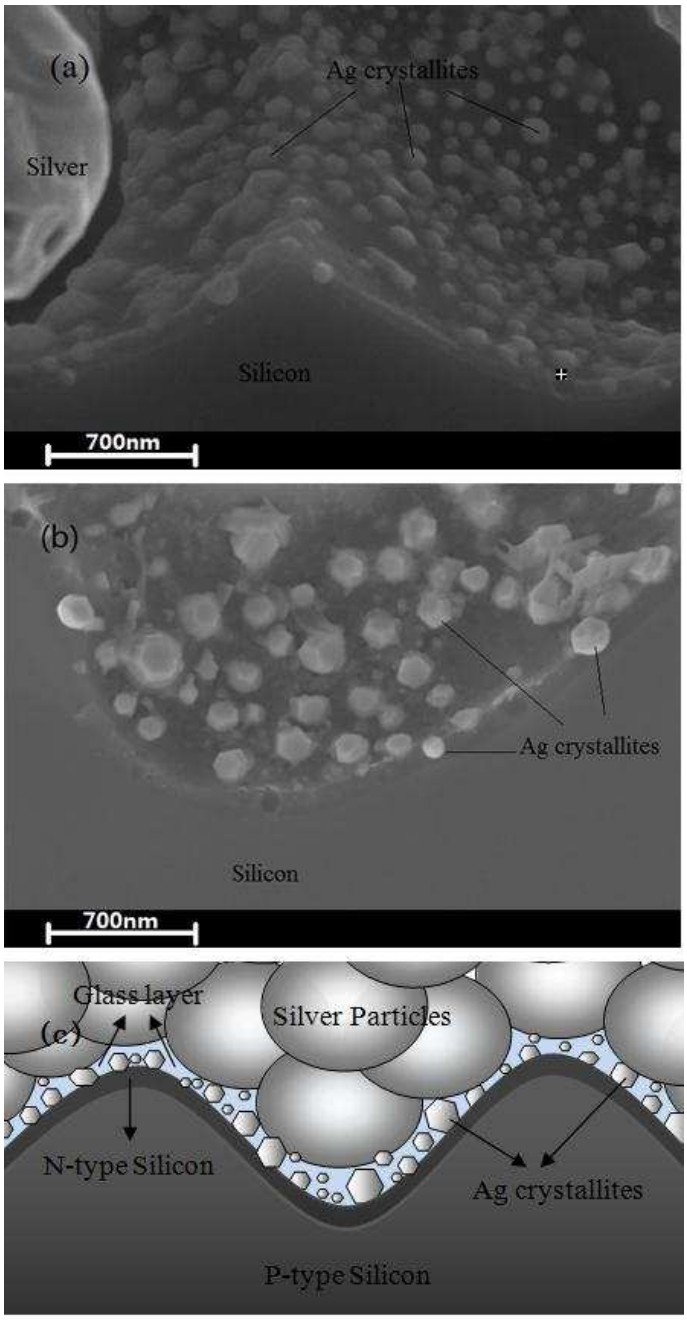

Figure 4

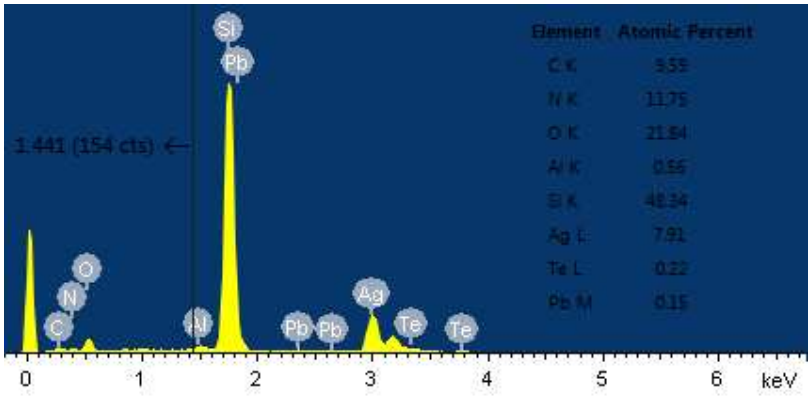

Figure 5

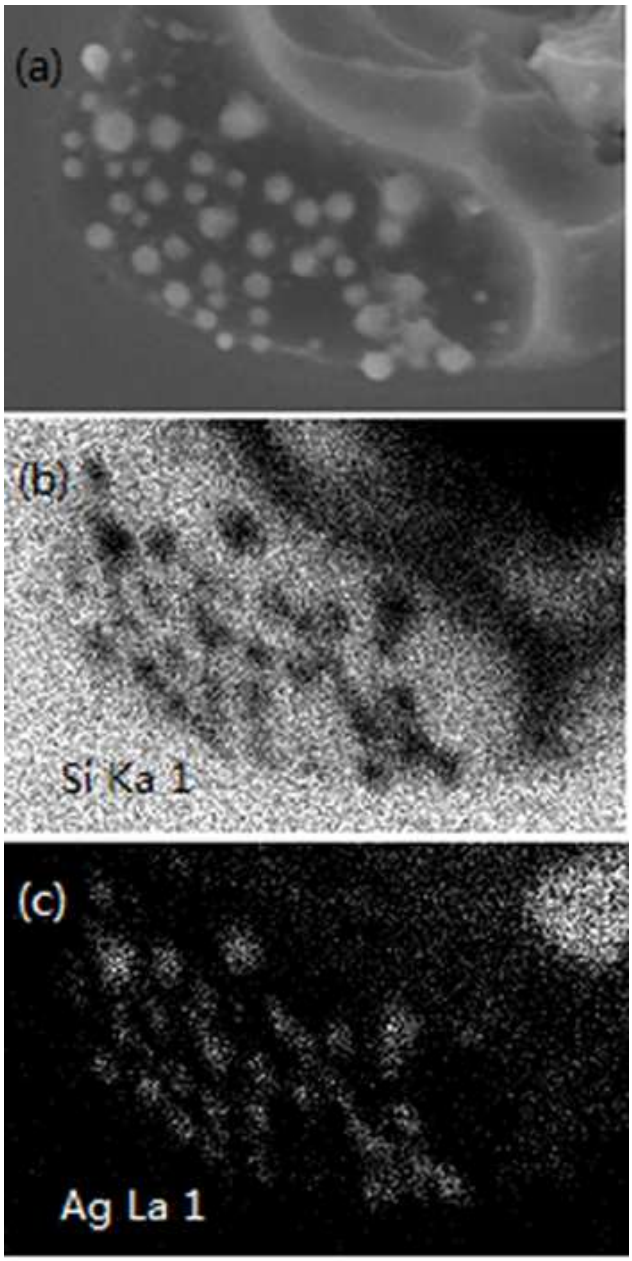

Figure 6